

photomorphogenesis (17). Here, we show that the enhanced stabilization of phyB-Pfr is responsible for the light-hypersensitive phenotypes in ARR4-overexpressing lines. Moreover, ARR4 contributes to this regulatory mechanism, and the ARR4:phyB interaction requires the extreme NH<sub>2</sub>-terminus domain of phyB. These results raise the question whether phyB is the cognate sensor kinase of ARR4 or whether it is the target of a two-component signaling system comprising ARR4. Because histidine kinase activity of phyB has not been reported and because *ARR4* gene expression is also induced by cytokinin (9), phyB may be the target of a hormone-modulated signaling system rather than the sensor kinase itself. The cytokinin receptor CRE1 is a functional sensor histidine kinase (19, 20), which might regulate the activity of ARR4. *Arabidopsis* seedlings expressing a nonphosphorylatable form of ARR4, display a hypersensitive phenotype to red light (21). This observation demonstrates the importance of phosphorylation of ARR4 for the modulation of phyB signaling. Therefore we propose that ARR4 may act as a signal module integrating both red light (*via* phyB) and hormone (cytokinin) signaling.

## References and Notes

- M. M. Neff, C. Fankhauser, J. Chory, *Genes Dev.* **14**, 257 (1999).
- S. Mathews, R. A. Sharrock, *Plant Cell Environ.* **20**, 666 (1997).
- F. Nagy, S. Kircher, E. Schäfer, *Semin. Cell Dev. Biol.* **11**, 505 (2000).
- K.-C. Yeh, S.-H. Wu, J. C. Lagarias, *Science* **277**, 1505 (1997).
- H. A. W. Schneider-Poetsch, B. Braun, S. Marx, A. Schaumburg, *FEBS Lett.* **281**, 245 (1991).
- K.-C. Yeh, J. C. Lagarias, *Proc. Natl. Acad. Sci. U.S.A.* **95**, 13976 (1998).
- P. Matsumura, J. J. Rydel, R. Linzmeier, D. Vacante, *J. Bacteriol.* **160**, 36 (1984).
- G. E. Schaller, D. Mathews, M. Griboskov, J. C. Walker, in *The Arabidopsis Book*, C. Somerville, E. Meyerowitz, Eds. (American Society of Plant Biologists, Rockville, MD, in press).
- I. Brandstatter, J. J. Kieber, *Plant Cell* **10**, 1009 (1998).
- A. Imamura *et al.*, *Proc. Natl. Acad. Sci. U.S.A.* **95**, 2691 (1998).
- T. D. Elich, J. Chory, *Plant Cell* **9**, 2271 (1997).
- T. Kunkel *et al.*, *Eur. J. Biochem.* **215**, 587 (1993).
- C.-M. Park, S.-H. Bhoo, P.-S. Song, *Semin. Cell Dev. Biol.* **11**, 449 (2000).
- J. Lohrmann *et al.*, *Mol. Genet. Genomics* **265**, 2 (2001).
- S. Kircher *et al.*, *Plant Cell* **11**, 1445 (1999).
- For details, supplementary material is available on Science Online at [www.sciencemag.org/cgi/content/full/294/5544/1108/DC1](http://www.sciencemag.org/cgi/content/full/294/5544/1108/DC1).
- K. Eichenberg, L. Hennig, A. Martin, E. Schäfer, *Plant Cell Environ.* **23**, 311 (2000).
- K. Eichenberg, thesis, University of Freiburg, Germany (1999).
- T. Inoue *et al.*, *Nature* **409**, 1060 (2001).
- T. Suzuki *et al.*, *Plant Cell Physiol.* **42**, 107 (2001).
- U. Sweere, thesis, University of Freiburg, Germany (2001).
- A. Nagatani *et al.*, *Cell Physiol.* **25**, 1059 (1985).
- S. Kircher *et al.*, *J. Cell Biol.* **144**, 201 (1999).
- We thank C. Fankhauser for the *PHYB* and *PHYB-101* cDNAs; L. Hennig for the *PHYA* construct; A. Nagatani, M. Furuya, and L. Nover for antibodies;

and the *Arabidopsis* Biological Resource Center, Ohio State University, for expressed sequence tag clones. This work was supported by a Sonderforschungsbereich grant to K.H. and E.S., and a Howard Hughes Medical Institute International Scholarship and a Human Frontier Science Program grant to

F.N. U.S. and K.E. were recipients of fellowships from the Landesgraduiertenförderung and the Evangelische Studentenwerk, respectively.

2 August 2001; accepted 19 September 2001

## Synaptotagmin Modulation of Fusion Pore Kinetics in Regulated Exocytosis of Dense-Core Vesicles

Chih-Tien Wang,<sup>1</sup> Ruslan Grishanin,<sup>2</sup> Cynthia A. Earles,<sup>1</sup> Payne Y. Chang,<sup>1</sup> Thomas F. J. Martin,<sup>2</sup> Edwin R. Chapman,<sup>1</sup> Meyer B. Jackson<sup>1\*</sup>

In the exocytosis of neurotransmitter, fusion pore opening represents the first instant of fluid contact between the vesicle lumen and extracellular space. The existence of the fusion pore has been established by electrical measurements, but its molecular composition is unknown. The possibility that synaptotagmin regulates fusion pores was investigated with amperometry to monitor exocytosis of single dense-core vesicles. Overexpression of synaptotagmin I prolonged the time from fusion pore opening to dilation, whereas synaptotagmin IV shortened this time. Both synaptotagmin isoforms reduced norepinephrine flux through open fusion pores. Thus, synaptotagmin interacts with fusion pores, possibly by associating with a core complex of membrane proteins and/or lipid.

The fusion pore represents a pivotal intermediate in Ca<sup>2+</sup>-triggered neurotransmitter exocytosis. Contact sites between the vesicle and the plasma membrane presumably contain special components capable of forming a fusion pore after the binding of Ca<sup>2+</sup>. The fusion pore has been likened to the channels that control ion flux across cell membranes (1), and like ion channels, single fusion pore activity can be observed in high-resolution electrical measurements (2–5). Whereas plasma membrane ion channels are formed by well-characterized proteins, the structural components of the fusion pore have yet to be identified. A molecule likely to be intimately associated with fusion pores is synaptotagmin, a synaptic vesicle protein that binds Ca<sup>2+</sup> and phospholipid (6). Genetic and biochemical studies have suggested a number of possible functions for synaptotagmin in vesicle trafficking and fusion (7–10). One appealing scenario is that soluble *N*-ethylmaleimide-sensitive factor attachment protein receptors (SNAREs) form fusion pores. These proteins catalyze the fusion of lipid

vesicles (11), and putative fusion pores formed by these proteins could be regulated by synaptotagmin through rapid Ca<sup>2+</sup>-stimulated binding to the SNARE complex (12). Here, we examined the role of synaptotagmin in specific steps of secretion in norepinephrine (NE)-secreting PC12 cells using amperometry to monitor release from individual dense-core vesicles.

When an amperometry electrode was positioned at the surface of a PC12 cell, exocytosis of a single vesicle registered as a spike of current as NE was oxidized at the electrode surface (3, 13) (Fig. 1). These spikes were elicited by depolarization, in this case induced by rapid local application of KCl (Fig. 1) (14). Responses to KCl were characterized by a latent period with no spikes, followed by a period of spikes at irregular intervals. Recordings such as these provide information about the kinetics of exocytosis, allowing us to compare control PC12 cells (Fig. 1A) with cells transfected with either synaptotagmin I (Fig. 1B), synaptotagmin IV (Fig. 1C) (15), or the  $\alpha$ 1A (P/Q-type) Ca<sup>2+</sup> channel (Fig. 1D). Because of the irregular nature of the release process in a single trial, we counted spikes after a given time interval and constructed normalized waiting time distributions (Fig. 1E). These plots provide an overall time course for secretion that is in

<sup>1</sup>Department of Physiology, University of Wisconsin Medical School, <sup>2</sup>Department of Biochemistry, University of Wisconsin, Madison, WI 53706, USA.

\*To whom correspondence should be addressed. E-mail: [mjackson@physiology.wisc.edu](mailto:mjackson@physiology.wisc.edu)

qualitative agreement with previous studies of dense-core vesicle secretion in PC12 cells (16–18). Synaptotagmin I did not alter the time course significantly. By contrast, secretion was reduced by synaptotagmin IV and enhanced by Ca<sup>2+</sup> channels. Thus, the level of secretion in PC12 cells falls in a range amenable to regulation in either direction.

The spike frequency (maximum slopes in Fig. 1E) was doubled by Ca<sup>2+</sup> channels, unchanged by synaptotagmin I, and reduced 2.6-fold by synaptotagmin IV (Fig. 1F). Each change in frequency was accompanied by a change in latency (time from onset of stimulation to first spike) in the opposite direction (Fig. 1G). Other spike properties such as amplitude and quantal size, which are not directly related to the kinetics of exocytosis, were not altered by synaptotagmin I or IV (19). The results with Ca<sup>2+</sup> channels indicate sensitivity to Ca<sup>2+</sup> current, but the reduction in exocytosis caused by synaptotagmin IV transfection cannot be explained by changes in Ca<sup>2+</sup> current. Ca<sup>2+</sup> current was unaffected by transfection with synaptotagmin I or IV (20). The mean peak Ca<sup>2+</sup> current elicited by voltage steps from –80 to +10 mV was 53 ± 17 pA in control cells (N = 6), 47 ± 10 pA

in cells transfected with synaptotagmin I (N = 7, P = 0.38), and 53 ± 11 pA in cells transfected with synaptotagmin IV (N = 7, P = 0.35). As expected, transfection with Ca<sup>2+</sup> channels increased Ca<sup>2+</sup> current to 104 ± 9 pA (N = 5, P < 0.05). The time constants for Ca<sup>2+</sup> current inactivation ranged from 350 to 450 ms for control and synaptotagmin-transfected cells and were statistically indistinguishable. Thus, although synaptotagmin is known to interact with Ca<sup>2+</sup> channels (21–23), no effect was observed here.

The vesicle size distribution is altered in *Drosophila* lacking synaptotagmin I (24). We examined the distribution of quantal size, as this should reflect dense-core vesicle size (provided that vesicular NE concentration remains the same). Spike area (cube root transformed to be proportional to vesicle diameter) appeared to be normally distributed and was indistinguishable between controls and synaptotagmin I or IV (19). Ca<sup>2+</sup> channel transfection produced a small but significant increase in spike amplitude and quantal size as well as a small shift in the distribution. PC12 cells contain a heterogeneous population of vesicles (25), and this analysis indi-

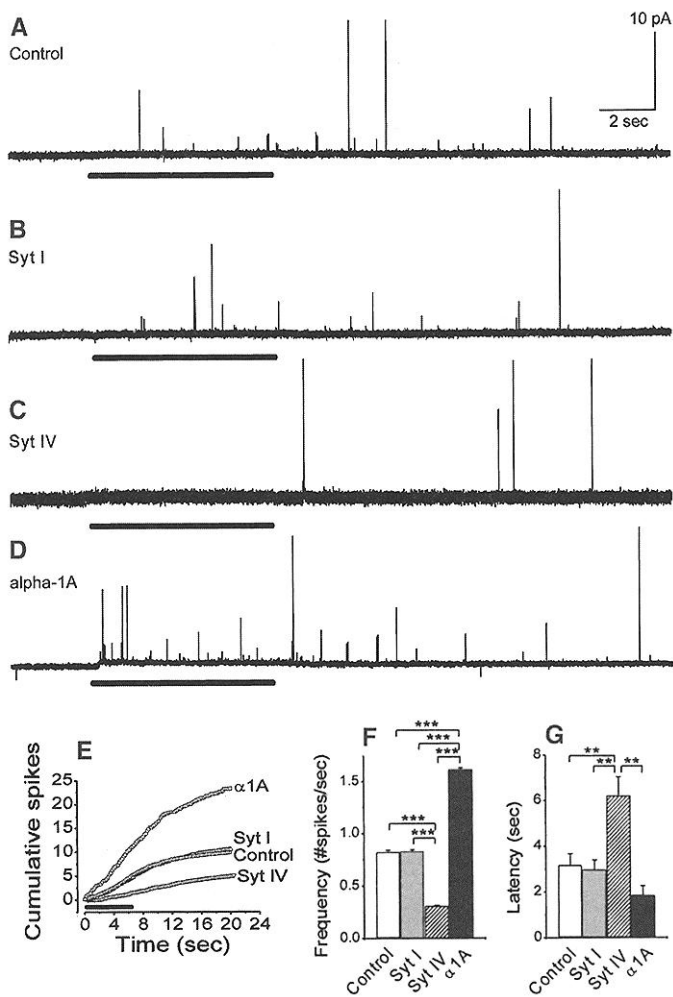
cated that synaptotagmin transfection did not redistribute vesicles between size groups.

The different vesicles of PC12 cells undergo exocytosis with different kinetics (16, 17). To determine whether transfected proteins were targeted to dense-core vesicles, we prepared fusion proteins of cyan fluorescent protein (CFP) linked to the NH<sub>2</sub>-terminus of synaptotagmin I and IV (26). Cells transfected with these constructs exhibited CFP fluorescence concentrated in highly mobile puncta, consistent with a location on vesicles. Ca<sup>2+</sup>-triggered exocytosis was readily seen in these cells. Cells were fixed and stained with antibodies against CFP and the dense-core vesicle protein chromogranin (Fig. 2). Chromogranin and synaptotagmin exhibited the same pattern of fluorescence, and overlays showed that both synaptotagmin I and IV colocalized with chromogranin (Fig. 2). Thus, both isoforms were targeted to dense-core vesicles.

If synaptotagmin participates in membrane fusion, then transfecting different isoforms should alter fusion pore kinetics. We therefore examined the “foot” current, which immediately precedes the steeply rising spike (Fig. 3A). Foot onset signals fusion pore opening, and feet are seen in association with ~80% of spikes ≥ 20 pA. The amplitude of ~3 pA was similar to that in chromaffin cells, but the duration was considerably shorter (3, 27). We examined the lifetimes of feet to determine whether synaptotagmin influences the stability of the fusion pore. As with ion channels (28, 29), the transitions of fusion pores are stochastic in nature, so we used lifetime distributions to characterize fusion pore kinetics (Fig. 3B). These were well fitted by a single exponential (P < 0.0001 for each fit), as previously reported (3). Thus, the open fusion pore can be represented by a single kinetic state. The time constant obtained from these exponential fits is equal to the mean open time, which was 1.38 ± 0.04 ms in control cells, 1.76 ± 0.06 ms with synaptotagmin I, and 0.97 ± 0.02 ms with synaptotagmin IV. These values are significantly different (Fig. 3C, left), indicating that exogenous synaptotagmin alters the stability of the fusion pore. Vesicles containing excess synaptotagmin I formed more stable fusion pores, and vesicles containing excess synaptotagmin IV formed less stable fusion pores. The lifetime of 1.70 ± 0.05 ms with Ca<sup>2+</sup> channels was similar to that with synaptotagmin I, suggesting that enhancing Ca<sup>2+</sup> entry and enhancing Ca<sup>2+</sup> sensing have similar effects on fusion pore dynamics.

The foot current amplitude, by analogy with the ion channels, can be influenced by the shape of the fusion pore and by the dynamics of very rapid transitions between per-

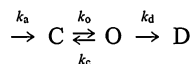
**Fig. 1.** Amperometric recordings of NE release from PC12 cells (depolarization with KCl indicated by bars). (A) Control cells. (B) Cells transfected with synaptotagmin I. (C) Cells transfected with synaptotagmin IV. (D) Cells transfected with α1A Ca<sup>2+</sup> channels. (E) Distributions of spike times for control, synaptotagmin I, synaptotagmin IV, and α1A. The distributions were normalized to the number of trials (42 for control, 30 for synaptotagmin I, 38 for synaptotagmin IV, and 11 for α1A). Mean (F) frequency and (G) spike latency. Frequency was calculated as the maximum slope from the plots in (E); first-spike latency was averaged from all recordings. Means are of >500 events from 11 to 42 cells, in experiments from two to eight transfections. \*\*, P < 0.01; \*\*\*, P < 0.001.



meation states.  $Ca^{2+}$  channels, synaptotagmin I, and synaptotagmin IV all reduced the foot amplitude (Fig. 3C, right). This suggests that these proteins either influence the structure of the fusion pore, possibly by narrowing or lengthening it, or modulate a dynamic pore-gating process that is too fast to see with our instrumentation.

The foot current is thought to terminate by fusion pore dilation, during which transmitter rapidly escapes from a vesicle in a spike of current. This phase of release is controlled by NE escape from an intravesicular matrix (27), as well as diffusion when exocytosis occurs at sites away from the electrode (30). Transfection with proteins altered spike shape (Fig. 4). Synaptotagmin IV accelerated the rise time (Fig. 4B) but left the decay times unchanged (Fig. 4, C and D). Slightly more than 50% of the spike decays were double exponential, with the fast component dominating.  $Ca^{2+}$  channels and synaptotagmin I had no effect on the rise time (Fig. 4B) but slowed the fast component of decay (Fig. 4C). The slow component of decay was markedly slowed by synaptotagmin I (Fig. 4D). MUNC18 was also recently reported to alter spikes, reducing the half-width and quantal size of spikes in chromaffin cells (31). Because spike shape and size are governed by events after fusion pore dilation, these results are not what one would expect for proteins involved in membrane trafficking. Thus, the factors controlling transmitter efflux after fusion pore dilation require further study.

Synaptotagmin I and IV both altered fusion pore lifetime (Fig. 3), indicating that this protein regulates the fusion step. Because our measurements are at the single-channel level, we used ideas developed from channel kinetics to interpret the results (28, 29). We consider assembly of a closed fusion pore, reversible opening and closing, and irreversible open pore dilation in a kinetic scheme.



The open state (O) produces foot current, and the dilating state (D) produces the spike.  $k_a$  is the assembly rate constant,  $k_o$  and  $k_c$  are the opening and closing rate constants, and  $k_d$  is the rate of entering the dilating state. The open-time distribution will then be a single exponential with a time constant:

$$\tau_{fp} = 1/(k_d + k_c)$$

Both  $k_d$  and  $k_c$  contribute to  $\tau_{fp}$ , because both processes terminate the open fusion pore state. According to this model, synaptotagmin I reduced the sum  $k_d + k_c$ , whereas synaptotagmin IV increased it.

Changes in  $k_a$ ,  $k_o$ ,  $k_d$ ,  $k_c$ , or the number of membrane-associated vesicles can all account for the changes in time course of exocytosis

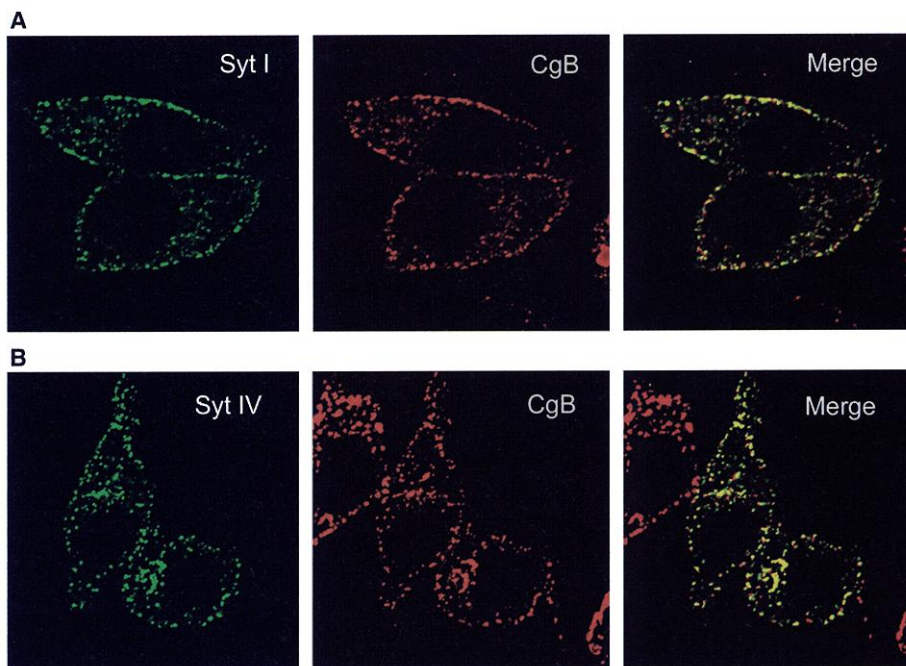


**Fig. 2.** Synaptotagmin on dense-core vesicles. CFP-tagged synaptotagmin and the dense-core vesicle protein chromogranin were visualized by double immunofluorescence (26) in cells transfected with CFP-synaptotagmin I (A) and CFP-synaptotagmin IV (B). CFP-synaptotagmin is shown as green (left) and chromogranin as red (center). Merged images (right) show colocalization as yellow. Cells that did not take up cDNA for the fusion protein stain only for chromogranin and appear red in the merged images.

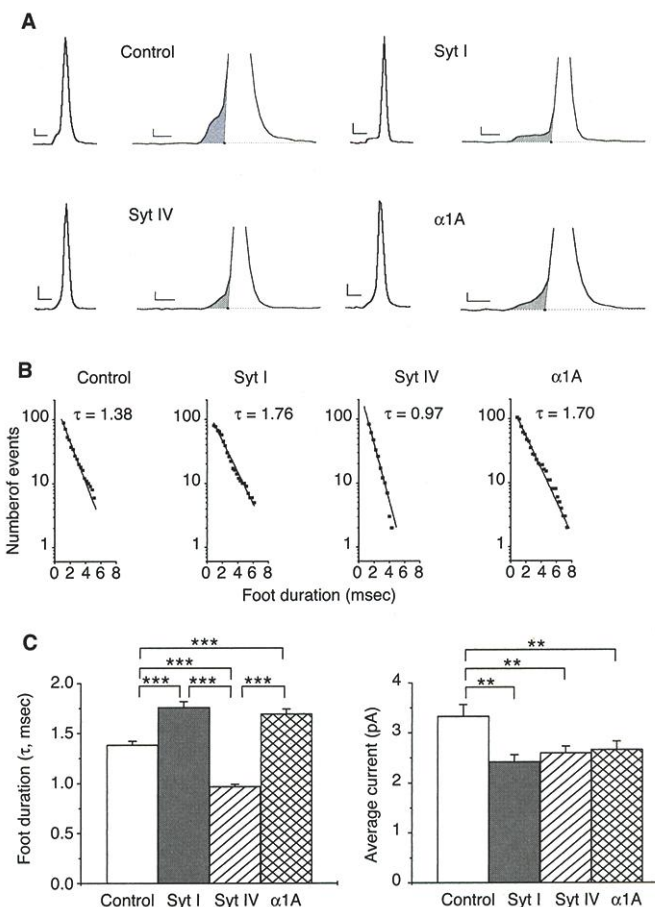


**Fig. 3.** (A) Foot current indicates fusion pore opening. Different scales illustrate the whole spike (left) and the foot (right). The foot regions (shaded) are delimited by the baseline and spike onset (scale bars: 10 pA, 2 ms, left; 5 pA, 1 ms, right). (B) Fusion pore open-time distributions. Single exponential fits yielded the mean open time,  $\tau$  ( $\tau_{fp}$  in text). (C)  $\tau$  (left) and mean NE flux (right). Flux was computed as foot area divided by duration. \*\*,  $P < 0.01$ ; \*\*\*,  $P < 0.001$ . All means were of  $\sim 100$  events.

in Fig. 1. Increasing  $k_c$  would make exocytosis slower by terminating more fusion pore openings without producing spikes, leaving stand-alone feet, which often elude detection (32). It is important that increasing  $k_c$  reduces the frequency and increases the latency, because it can also account for the reduction in  $\tau_{fp}$ . This provides a simple explanation for the direction of the observed changes produced by synaptotagmin IV in three different measurements. Synaptotagmin I increased the fusion pore lifetime (Fig. 3) but left the latency and frequency unchanged (Fig. 1). According to the above model, this would result from 20% reductions in both  $k_d$  and  $k_c$ . This will not alter spike frequency or latency (Fig. 1, F and G) because the fraction of open fusion pores that dilate,  $k_d/(k_c + k_d)$ , remains unchanged. Thus, the results of both synaptotagmin I and IV are most parsimoniously explained by changes in rate constants directly associated with the open fusion pore.

PC12 cells express synaptotagmin I (33, 34) and IX (35) and contain synaptotagmin III mRNA (36). Transfection with synaptotagmin I should increase the ratio of synaptotagmin I to other isoforms and may increase the number of copies of synaptotagmin per vesicle as well. The parallel changes in  $k_d$  and  $k_c$  just discussed for synaptotagmin I would then reflect these changes. Enhancing  $Ca^{2+}$  entry with extra  $Ca^{2+}$  channels altered the stability of the fusion pore in the same way as

extra synaptotagmin I, as expected if synaptotagmin I acts as a  $Ca^{2+}$  sensor. Synaptotagmin IV levels are normally very low in PC12 cells (34). In light of the weak  $Ca^{2+}$  binding of this protein (37), the reduced exocytosis seen with synaptotagmin IV further supports synaptotagmin's role as a  $Ca^{2+}$  sensor. Overexpression of synaptotagmin IV in *Drosophila* reduces synaptic transmission (38), and this may reflect the reduction in  $Ca^{2+}$ -triggered fusion observed here.

Synaptotagmin influences the stability of open fusion pores and is therefore likely to be intimately associated with a molecular complex that performs the function of fusing vesicle and plasma membranes. Changes in fusion pore dynamics have recently been proposed to play a role in synaptic plasticity (39), and the control of synaptic vesicle fusion pores by synaptotagmin could provide a molecular mechanism. Synaptotagmin oligomerizes (40) and binds lipids (6), syntaxin (41), SNAP-25 (42), and the SNARE complex (12), all in a  $Ca^{2+}$ -dependent manner. Because SNARE proteins fuse membranes (11), the synaptotagmin-mediated alteration in fusion pore open time may represent a functional consequence of these interactions. Mutations in synaptotagmin that impair  $Ca^{2+}$ -triggered lipid binding (9) and oligomerization (10) reduce synaptic transmission, and the present approach offers a means of assessing whether these mutations act

through a change in fusion pore kinetics. Future studies on how the control of fusion pores by synaptotagmin is regulated by  $Ca^{2+}$  and SNARE proteins may provide a precise picture of how this protein transduces  $Ca^{2+}$  signals during excitation-secretion coupling.

References and Notes

- M. Lindau, W. Almers, *Curr. Opin. Neurobiol.* **7**, 509 (1995).
- L. J. Breckenridge, W. Almers, *Nature* **328**, 814 (1987).
- R. H. Chow, L. von Rüden, E. Neher, *Nature* **356**, 60 (1992).
- G. Alvarez de Toledo, R. Fernandez-Chacon, J. M. Fernandez, *Nature* **363**, 554 (1993).
- D. Bruns, R. Jahn, *Nature* **377**, 62 (1995).
- N. Brose, A. G. Petrenko, T. C. Südhof, R. Jahn, *Nature* **256**, 1021 (1992).
- T. L. Schwarz, *Curr. Opin. Neurobiol.* **4**, 633 (1994).
- T. E. Lloyd, H. J. Bellen, in *Neurotransmitter Release*, H. Bellen, Ed. (Oxford Univ. Press, Oxford, 2000), pp. 352-388.
- R. Fernandez-Chacon *et al.*, *Nature* **410**, 41 (2001).
- J. T. Littleton *et al.*, *J. Neurosci.* **21**, 1421 (2001).
- T. Weber *et al.*, *Cell* **92**, 759 (1998).
- A. F. Davis *et al.*, *Neuron* **24**, 363 (1999).
- R. M. Wightman *et al.*, *Proc. Natl. Acad. Sci. U.S.A.* **88**, 10754 (1991).
- Amperometry recording used 5- $\mu$ m carbon fibers and a VA-10 amplifier (ALA Instruments) at a polarization of 650 mV [R. H. Chow, L. von Rüden, in *Single-Channel Recording*, B. Sakmann, E. Neher, Ed. (Plenum, New York, 1995), pp. 245-275]. Cells were bathed in 150 mM NaCl, 4.2 mM KCl, 1 mM  $NaH_2PO_4$ , 0.7 mM  $MgCl_2$ , 2 mM  $CaCl_2$ , and 10 mM Hepes (pH 7.4) at  $\sim 22^\circ C$ . Current was low-pass filtered at 1 kHz and digitized at 4 kHz by a PC running PCLAMP 8 (Axon Instruments). Cells were plated at  $1.2 \times 10^5$  cells per 35 mm dish and loaded by bathing in 1.5 mM NE and 0.5 mM ascorbate 1 day before experiments. Secretion was induced by pressure ejection of 105 mM KCl/5 mM NaCl in the cell bathing solution from a  $\sim 2$ - $\mu$ m tipped micropipette  $\sim 10$   $\mu$ m away. Amperometry records were analyzed with a program written in this laboratory to extract foot information according to the criteria of Chow and von Rüden. Spikes exceeding five times the background noise ( $\sim 0.4$  pA) were analyzed. Feet were analyzed for spikes  $\geq 20$  pA. Error bars are standard errors.
- PC12 cells were cultured [J. C. Hay, T. F. J. Martin, *J. Cell Biol.* **119**, 139 (1992)] in Dulbecco's modified essential medium, with glucose (4.5 mg/ml),  $NaHCO_3$  (3.7 mg/ml), 5% horse serum, and 5% iron-supplemented calf serum, in 10%  $CO_2$ -air at  $37^\circ C$ . Cells were transfected with 50  $\mu$ g of DNA in 120 mM KCl, 0.15 mM  $CaCl_2$ , 10 mM  $KH_2PO_4$ , 2 mM EGTA, 5 mM  $MgCl_2$ , 2 mM Mg-adenosine triphosphate (ATP), 5 mM glutathione, and 2.5 mM Hepes (pH 7.6). An Invitrogen electroporator was set at 1000  $\mu$ F and 330 V. cDNAs encoding synaptotagmin I (G374) (43), synaptotagmin IV (44), and P/Q  $Ca^{2+}$  channels (45) were subcloned into pRES2-EGFP (Clontech) with Nhe I and Bam HI for synaptotagmin I, Nhe I and Sma I for synaptotagmin IV, and Sal I and Bam HI for P/Q  $Ca^{2+}$  channel. Experiments were performed 60 to 96 hours after transfection. Transfected cells ( $\sim 30\%$  efficiency) were selected by green fluorescent protein (GFP) fluorescence. Control cells were transfected with vector lacking a second insert. Control and untransfected cells were similar.
- H. Kasai *et al.*, *J. Physiol.* **494**, 53 (1996).
- T. Kishimoto *et al.*, *J. Physiol.* **533**, 627 (2001).
- C. A. Earles, J. Bai, P. Wang, E. R. Chapman, *J. Cell Biol.*, in press.
- Supplementary data are available on Science Online at [www.sciencemag.org/cgi/content/full/294/5544/1111/DC1](http://www.sciencemag.org/cgi/content/full/294/5544/1111/DC1).
- $Ca^{2+}$  current was measured by patch clamp [O. P. Hamill *et al.*, *Pflügers Arch.* **391**, 85 (1981)] with an EPC-7 amplifier (Instrutech). Borosilicate patch pipettes of 3 to 7 megaohms were filled with 90 mM

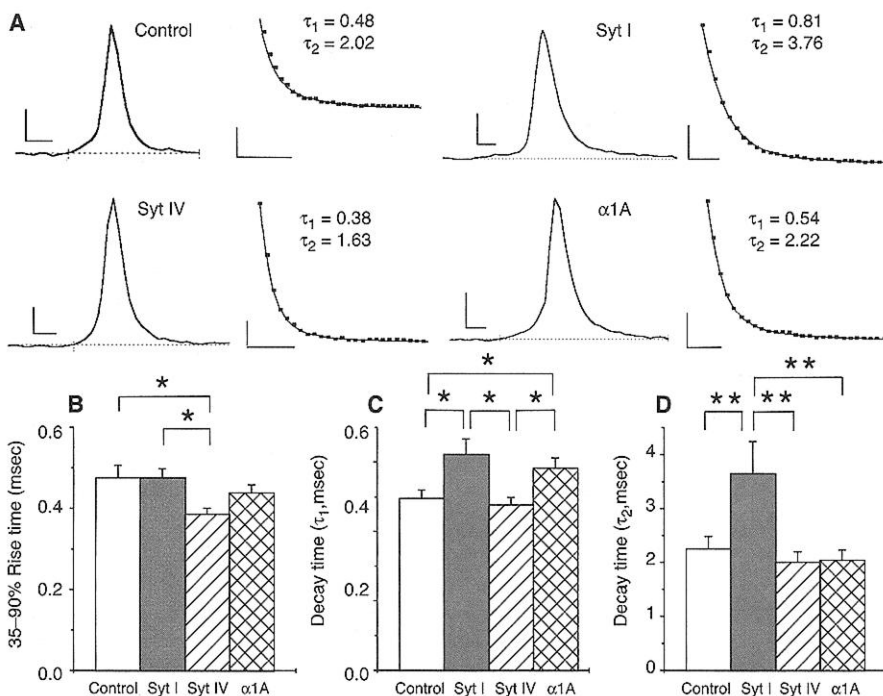


Fig. 4. (A) Spike shapes and decays. Spikes are shown alongside double exponential fits to the decay phase (scale bars: 10 pA, 1 ms). (B) Spike rise times (35 to 90%). (C) The time constant for the fast component of spike decay,  $\tau_1$  (decays of single exponential fits were similar to the decays of the fast component of double exponential fits, so the values were combined). (D) Time constants for the slow component of decay,  $\tau_2$ , from decays that were double exponential. \*,  $P < 0.05$ ; \*\*,  $P < 0.01$  [ $N = \sim 100$  in (B),  $\sim 100$  in (C), and  $\sim 25$  in (D)].

*N*-methylglucamine, 20 mM TEA-Cl, 0.2 mM EGTA, 2 mM MgCl<sub>2</sub>, 20 mM Na<sub>2</sub>-creatine phosphate, 5 mM Mg-ATP, and 0.1 mM guanosine triphosphate, and 10 Hepes (pH 7.35). The bathing solution was 105 mM NaCl, 20 mM CaCl<sub>2</sub>, 1.5 mM MgSO<sub>4</sub>, 15 mM glucose, 0.003 mM tetrodotoxin, and 5 mM Hepes (pH 7.35).

21. N. Charvin *et al.*, *EMBO J.* **16**, 4591 (1997).

22. O. Wiser, D. Tobi, M. Trus, D. Atlas, *FEBS Lett.* **404**, 203 (1997).

23. D. K. Kim, W. A. Catterall, *Proc. Natl. Acad. Sci. U.S.A.* **94**, 14782 (1997).

24. N. E. Reist *et al.*, *J. Neurosci.* **18**, 7662 (1998).

25. R. Bauerfeind, A. Regnier-Vigouroux, T. Flatmark, W. B. Huttner, *Neuron* **11**, 105 (1993).

26. Cells were permeabilized with 0.3% Triton X100, fixed in paraformaldehyde, blocked in 10% fetal bovine serum (FBS) in phosphate-buffered saline (PBS) for 1 hour, and incubated with primary antibodies diluted in 10% FBS for 1 hour. CFP-tagged protein was detected with rabbit polyclonal antibody to GFP (Panvera). Chromogranin B was detected with a mouse monoclonal antibody (generously provided by W. Huttner). Cells were washed and stained with secondary antibodies (fluorescein-conjugated goat

antibody to rabbit for CFP and Texas red-conjugated goat antibody to mouse for chromogranin) for 1 hour. After four washes in PBS, cover slips were mounted and examined with a Bio-Rad MRC 600 confocal system. Subcloning into the pECFP-C1 vector (Clontech) used Eco RI and Bam HI for synaptotagmin I and Hind III and Kpn I for synaptotagmin IV. Transfection was as in (15).

27. T. J. Schroeder *et al.*, *Biophys. J.* **70**, 1061 (1996).

28. D. Colquhoun, A. G. Hawkes, in *Single-Channel Recording*, B. Sakmann, E. Neher, Eds. (Plenum, New York, 1995), pp. 397-482.

29. M. B. Jackson, *Methods Enzymol.* **207**, 729 (1992).

30. M. Haller, C. Heinemann, R. H. Chow, R. Heidelberger, E. Neher, *Biophys. J.* **74**, 2100 (1998).

31. R. J. Fisher, J. Pevsner, R. D. Burgoyne, *Science* **291**, 875 (2001).

32. Z. Zhou, S. Mislis, R. H. Chow, *Biophys. J.* **70**, 1543 (1996).

33. Y. Shoji-Kasai *et al.*, *Science* **256**, 1820 (1992).

34. G. D. Ferguson, D. M. Thomas, L. A. Elferink, H. R. Herschman, *J. Neurochem.* **72**, 1821 (1999).

35. A. Hudson, M. Birnbaum, *Proc. Natl. Acad. Sci. U.S.A.* **92**, 5895 (1995).

36. M. Mizuta *et al.*, *J. Biol. Chem.* **269**, 11675 (1994).

37. C. von Poser, K. Ichtchenko, X. Shao, J. Rizo, T. Sudhof, *J. Biol. Chem.* **272**, 14314 (1995).

38. J. T. Littleton, T. L. Serano, G. M. Rubin, B. Ganetzky, E. R. Chapman, *Nature* **400**, 757 (1999).

39. S. Choi, J. Klingauf, R. W. Tsien, *Nature Neurosci.* **3**, 330 (2000).

40. E. R. Chapman, S. An, J. M. Edwardson, R. Jahn, *J. Biol. Chem.* **271**, 5844 (1996).

41. E. R. Chapman, P. I. Hanson, S. An, R. Jahn, *J. Biol. Chem.* **270**, 23667 (1995).

42. R. R. Gerona, E. C. Larsen, J. A. Kowalchuk, T. F. Martin, *J. Biol. Chem.* **275**, 6328 (2000).

43. R. C. Desai *et al.*, *J. Cell Biol.* **150**, 1125 (2000).

44. L. Vician, I. K. Lim, G. Ferguson, M. Baudry, H. R. Herschman, *Proc. Natl. Acad. Sci. U.S.A.* **92**, 2164 (1995).

45. P. T. Ellinor *et al.*, *Nature* **363**, 455 (1993).

46. Supported by grants from NIH to M.B.J. and T.F.J.M. and by grants from NIH, AHA, and the Milwaukee Foundation to E.R.C. E.R.C. is a Pew Scholar.

2 July 2001; accepted 21 September 2001

## Localization of Long-Term Memory Within the *Drosophila* Mushroom Body

Alberto Pascual and Thomas Pr at\*

The mushroom bodies, substructures of the *Drosophila* brain, are involved in olfactory learning and short-term memory, but their role in long-term memory is unknown. Here we show that the *alpha-lobes-absent (ala)* mutant lacks either the two vertical lobes of the mushroom body or two of the three median lobes which contain branches of vertical lobe neurons. This unique phenotype allows analysis of mushroom body function. Long-term memory required the presence of the vertical lobes but not the median lobes. Short-term memory was normal in flies without either vertical lobes or the two median lobes studied.

The organization of the *Drosophila* brain, which shows highly organized and specialized structures despite its small size, in combination with its sophisticated behavioral repertoires and powerful molecular genetic tools render this organism a model of choice for the study of integrative brain functions, such as associative learning and memory. The mushroom bodies (MBs) constitute a prominent bilateral structure of the insect brain. The MBs are formed and rearranged sequentially during embryonic and postembryonic development (1-3). In adult *Drosophila*, they are composed of about 5000 neurons, which receive, through the calyx, olfactory inputs from the antennal lobes. The MBs are essential for associative learning and memory (4-6). Several proteins involved in learning and short-term memory are detected at high levels in the MBs (7), and chemical ablation of

*Drosophila* MBs abolishes olfactory learning (6). Synaptic transmission from the MBs is required for retrieval of short-term memories but not for acquisition or storage (8, 9). With intensive and spaced training, *Drosophila* can also display long-term memory (LTM), which depends on protein synthesis after the conditioning paradigm (10). We have now tested whether *Drosophila* MBs are involved in LTM formation.

Three categories of MB intrinsic neurons (Kenyon cells), associated with five sets of lobes, have been described (Fig. 1A) (1, 11). Two types of neurons branch to give rise to a vertical and a median lobe ( $\alpha/\beta$  lobes and  $\alpha'/\beta'$  lobes, respectively). The third type composes the median  $\gamma$  lobe. Uniquely identifiable efferent neurons originate from specific parts of the medial and vertical lobes, and send their axons to characteristic regions of the forebrain (12). Afferents from the forebrain also invade specific parts of the lobes (12). The implication of this architecture, which also characterizes other insect MBs (13), suggests that the lobes are not identical and may support quite distinct functions.

Genetic characterization of the *alpha-lobes-absent (ala)* mutant, which shows abnormal MBs, was previously reported (14). The original mutation corresponds to the insertion of a P-element and is recessive. Phenotypic revertants as well as new mutant alleles were produced by excision of the P-element (14). We reassessed the *ala* brain defect using the *GALA-OK107* enhancer-trap line (15), which labels all five lobes (Fig. 1), and the antibody to FasciilinII (FasII), which strongly labels  $\alpha/\beta$  lobes and weakly labels  $\gamma$  lobes (11, 16). Three batches of brain analyses showed that  $10.5 \pm 2.8\%$  of *ala* individuals possessed all five lobes in both hemispheres,  $36 \pm 2.4\%$  lacked the  $\beta$  and  $\beta'$  lobes in both hemispheres, and  $4.5 \pm 1.1\%$  lacked  $\alpha$  and  $\alpha'$  vertical lobes. The remaining flies showed different combinations of phenotypes in the left and right hemisphere. *ala* flies without vertical lobes also showed a fusion of the left and right  $\beta$  and  $\beta'$  lobes (Fig. 1C). This fusion phenotype is also observed in a fraction of *ala* flies with all lobes present ( $3.6 \pm 1.4\%$  of total) (16). A similar phenotype distribution was observed in *ala/Df(1)4b18* individuals (17).  $\gamma$  lobes appeared to be normal in *ala* mutants. This observation was reinforced by the fact that in second instar larvae *ala* mutants possessed normal vertical and median  $\gamma$  projections (18).

The *ala* mutant was trained to associate an odor with electric shocks by using three different experimental paradigms (19, 20): (i) a single training cycle protocol to induce short-term memory (21); (ii) an intensive spaced conditioning protocol, consisting of 10 individual training sessions with a 15-min rest interval between each session, to induce LTM (10); and (iii) a massed conditioning protocol, consisting of 10 consecutive training sessions without rest, to induce 24-hour memory but not protein-synthesis dependent LTM (10).

Developpement, Evolution, Plasticit  du Syst me Nerveux, CNRS, 1 Avenue de la Terrasse, 91190 Gif-sur-Yvette, France.

\*To whom correspondence should be addressed. E-mail: preat@iaf.cnrs-gif.fr